

# Phonon anomaly, central peak, and microstructures in Ni<sub>2</sub>MnGa

A. Zheludev, S. M. Shapiro, and P. Wochner  
*Brookhaven National Laboratory, Upton, New York 11973*

A. Schwartz, M. Wall, and L. E. Tanner  
*Lawrence Livermore National Laboratory, Livermore, California 94550*  
 (Received 12 December 1994)

Inelastic neutron scattering and transmission electron microscopy have been used to study a single crystal of the Ni<sub>2</sub>MnGa shape-memory ferromagnetic Heusler alloy in a wide temperature range above the martensitic phase transformation at  $T_M = 220$  K. Significant, though incomplete, softening in the  $[\zeta\zeta 0]$  TA<sub>2</sub> phonon branch has been observed at a wave vector  $\zeta_0 \approx 0.33$ . The anomaly in the dispersion curve is shown to persist at high temperature, even above the Curie point. A temperature-dependent peak in the elastic diffuse scattering is also present at the same wave vector  $\zeta_0$ , which develops into a Bragg peak representative of an intermediate phase between the high-temperature Heusler and the low-temperature martensitic structures.

## I. INTRODUCTION

Many metallic alloys are known to undergo a martensitic phase transition, a displacive, diffusionless, first-order transformation from the symmetric high-temperature parent phase to a low-symmetry martensite structure at low temperature.<sup>1</sup> These phase transitions are, as a rule, associated with phonon anomalies in the parent phase. Particularly, in bcc materials the  $[\zeta\zeta 0]$  TA<sub>2</sub> mode with displacement along  $[1\bar{1}0]$  softens at a certain wave vector  $\zeta_0$  which is close to a reciprocal-lattice vector of the low-temperature structure. Extensive studies of Ni-Ti-Fe (Ref. 2) and Ni-Al (Ref. 3) alloys provided new insight on the relation of these phonon anomalies to the martensitic transformation and precursor phenomena. Experimental results were found to be in excellent agreement with theoretical calculations which attribute the phonon softening to electron-phonon coupling and specific nesting properties of the Fermi surface.<sup>4,5</sup> Nevertheless, the rich phenomenon of martensitic transformations is still not completely understood and investigation of other model systems is required to move further.

One interesting candidate for study is the Ni<sub>2</sub>MnGa intermetallic shape-memory alloy, which, among the large variety of ferromagnetic Heusler alloys, is the only one known to undergo a martensitic phase transition ( $T_M \approx 200$  K). Thermally and stress-induced martensite structures have been investigated in this system by x-ray diffraction, ultrasound measurements, and electron microscopy.<sup>6-8</sup> The thermal martensite structure was found to be roughly tetragonal,  $c/a = 0.94$ , with long-period modulations parallel to the basal plane (001) with a 5-plane periodicity. Recently, thermal diffuse x-ray scattering experiments<sup>9</sup> have indicated the presence of soft acoustic modes in the high-temperature phase. One immediate question is whether the phase transition and the phonon anomalies are in any way related to the ferromagnetic long-range order, as is the case in several

other magnetically ordered alloys.<sup>10,11</sup>

Herein we report an inelastic neutron scattering study of the fcc parent phase of Ni<sub>2</sub>MnGa in a wide temperature range. Significant  $[\zeta\zeta 0]$  TA<sub>2</sub> phonon softening was observed at a wave vector  $\zeta_0 \approx 0.33$ . The softening is not complete, i.e., the phonon frequency remains finite even as the transition temperature is approached. The anomaly was found to persist above the Curie point. This rules out its magnetoelastic origin. Strong temperature-dependent elastic scattering was observed at wave vectors close to  $\zeta_0$ , which develops into a Bragg peak of an intermediate phase as the martensitic transition temperature is approached.

## II. EXPERIMENT

At room temperature Ni<sub>2</sub>MnGa has a fcc L2<sub>1</sub> Heusler structure (space group  $Fm\bar{3}m$ , No. 225), the cell constant being 5.822 Å.<sup>6</sup> Due to the closeness of atomic x-ray scattering factors of the constituent elements, an alternative description of the structure, namely bcc A2 with  $a_{bcc} = \frac{1}{2}a_{fcc}$ , may be found in literature. Throughout this paper the (correct) fcc notation will be used. A single crystal was grown by the Bridgman method at Ames Laboratory particularly for this experiment. The 7 cm long sample had the shape of a half cylinder, 1.5 cm in diameter. The longer dimension was identified as  $[111]$ .

The sample was mounted on the H7 triple axis spectrometer at the high flux beam reactor at Brookhaven National Laboratory in a high-temperature Displex refrigerator. It was aligned to have the (100) plane coincide with the scattering plane of the spectrometer. The measurements were performed in the temperature range 230–400 K. The sample turned out to be composed of two crystallites, the mosaic spread was found to be of the order of 1°. The neutron scattering experiments were performed with a fixed final energy  $E_f =$

13.5 meV. Pyrolytic graphite PG(002) reflections were used for monochromator and analyzer.  $20' - 20' - 20' - 80'$  and  $10' - 10' - 10' - 80'$  collimations were used yielding an energy resolution of  $\delta E = 0.62$  meV and  $\delta E = 0.48$  meV full width at half maximum at  $\Delta E = 0$ , respectively. A pyrolytic graphite filter was positioned in front of the detector. Both constant- $Q$  and constant- $E$  scans were used to measure the phonon cross section.

Conventional electron microimages (amplitude contrast) and selected-area electron diffraction patterns were obtained with the standard JEOL 200 CX instrument equipped with double-tilt heating and cooling stages at Lawrence Livermore National Laboratory. High-resolution imaging (phase contrast), which is limited to room temperature, was carried out on the JEOL top-entry 200 CX and ARM instruments at the National Center for Electron Microscopy at the Lawrence Berkeley Laboratory.

### III. RESULTS AND DISCUSSION

The martensitic phase transition temperature  $T_M \approx 220$  K of the sample was estimated from the splitting of the [220] Bragg peak which occurs at 212 K on cooling and 228 K on warming up, thus showing a significant temperature hysteresis. The phase transition seems to be completely reversible. The Curie temperature  $T_C \approx 380$  K was determined from the increase of the [200] Bragg intensity on passing from the paramagnetic to the ordered state.

We concentrated our studies on the temperature dependence of the inelastic scattering of the  $[\zeta\zeta 0]$   $TA_2$  phonon branch. This mode, for  $\zeta \rightarrow 0$ , corresponds to the elastic constant  $c' = \frac{1}{2}(c_{11} - c_{12})$ , which is known to be anomalously low in bcc metals.<sup>12</sup> Limited data were collected for LA phonons propagating in the same direction and for the  $[\zeta 00]$  TA modes. In the entire temperature and  $q$  range the phonons are well defined. Figure 1 shows

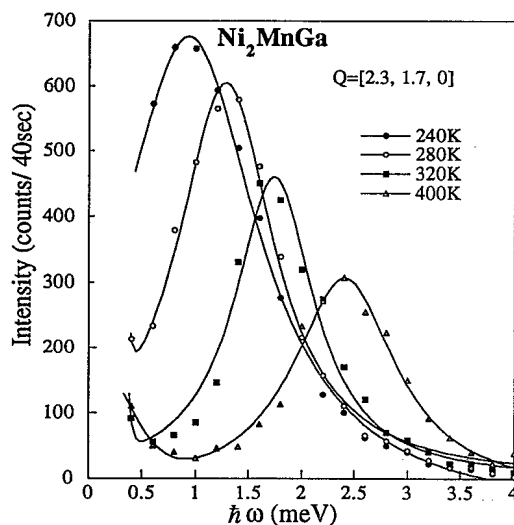


FIG. 1. Inelastic neutron scattering spectra for the  $[\zeta\zeta 0]$   $TA_2$ ,  $\zeta = 0.3$  phonon measured at several temperatures above  $T_M$ .

some representative spectra measured at different temperatures and already reveals the decrease of the phonon energy as the temperature approaches  $T_M$ .

Phonon dispersion curves measured at 370 and 270 K are shown in Fig. 2(a). The most prominent feature is the wiggle in the  $[\zeta\zeta 0]$   $TA_2$  branch, which deepens with decreasing temperature, resulting in a distinct minimum at  $\zeta_0 \approx 0.33$  below 300 K. The way the dip evolves is shown in Fig. 2(b). Several points should be emphasized here. (i) The wiggle is still present at  $T = 400$  K, i.e., above the Curie temperature. (ii) Even though the soft mode frequency decreases by a factor of 3 as  $T \rightarrow T_M$ , it never softens completely, i.e., its energy remains finite. (iii) It was observed that below  $T_1 \approx 260$  K, the soft mode frequency starts to *increase* on cooling. Note that  $T_1$  is nearly 40 K higher than the actual (i.e., bulk) martensitic

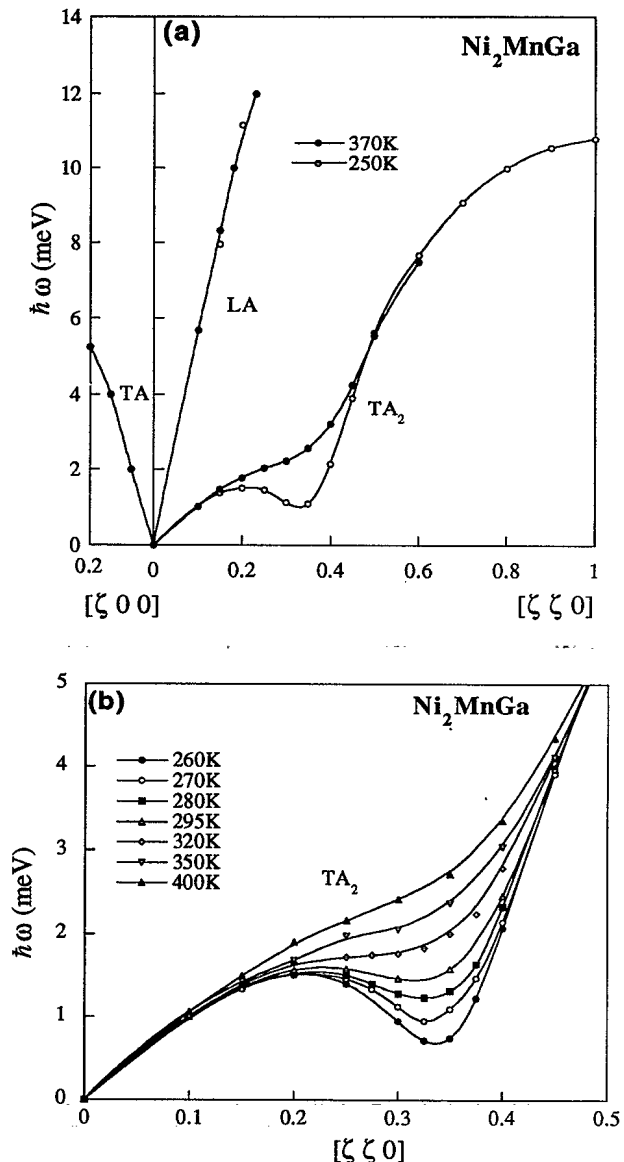


FIG. 2. (a) Partial acoustic phonon dispersion curves measured for  $Ni_2MnGa$  at 270 and 370 K. (b) Temperature dependence of the anomaly in the  $[\zeta\zeta 0]$   $TA_2$  branch.

transition temperature  $T_M$ . This suggests that between  $T_1$  and  $T_M$  another phase may develop and coexist with the parent phase.

Associated with the overall low energy of the dispersion curve and its anomalous dip at  $\zeta_0$  is an elastic, diffuse, central peak scattering, which develops as  $T \rightarrow T_M$ . Two significant effects are seen in the elastic scans along the  $[\zeta\zeta 0]$  direction with transverse polarization that are presented in Fig. 3. The first is diffuse scattering that diverges as  $\zeta \rightarrow 0$ , and the second, more pronounced effect is a satellite peak at  $\zeta_0$ . Both their intensities increase with decreasing temperature as shown Fig. 3(a). No other features appear up to the zone boundary; in particular, the peak at  $\zeta = 0.46$ , which was observed in

x-ray scattering experiments,<sup>9</sup> was not found.

Above  $T_1$  the satellite peak is broad in  $q$  space (the width  $\Delta q \approx 0.15 \text{ \AA}^{-1}$  is  $T$  independent). Energy scans over the entire temperature range show that the energy width of the elastic scattering is resolution limited. These scattering effects and their temperature dependence were also observed with electron diffraction. The room-temperature  $[001]$  zone-axis pattern in Fig. 4(a) shows  $\langle\zeta\zeta 0\rangle$  streaks emanating from each of the Bragg peaks and the satellites at  $\zeta \approx 0.33$  (note: only transverse effects are real; double diffraction accounts for the presence of radial scattering under these highly symmetric diffraction conditions<sup>13,14</sup>). The narrow energy width observed in the neutron experiment indicates that the elastic scattering is defect induced and directly related to the reduction of phonon frequencies as explained by the model proposed by Axe, Shirane, and Riste<sup>15</sup> and Halperin and Varma.<sup>16</sup> The corresponding microstructure [Fig. 4(b)] was imaged at room temperature by conventional or amplitude contrast transmission electron microscopy (CTEM), and has the characteristic form of the well-known "tweed" strain contrast.<sup>3,13,14</sup> This dense array of diffuse striations lying along  $\langle 110 \rangle$  lattice directions is related to the  $\langle\zeta\zeta 0\rangle$  streaks (Huang diffuse scattering) associated with the presence of localized long-wavelength shear strains of  $\{110\}\langle\bar{1}10\rangle$  type. The structural detail related to the  $\langle\zeta_0\zeta_0 0\rangle$  satellites can only be resolved by high-resolution, multibeam phase contrast imaging (HRTEM) (Refs. 3, 13, 14, and 17) and these local atomic configurations are seen in Fig. 4(c). The normal (unstrained) image of the  $L2_1$  structure in this orientation is a square pattern of sharply aligned white dots corresponding to atomic columns lying in  $\{220\}$  planes.<sup>3,17</sup> In the micrograph, we see that this pattern is severely perturbed. The result is an inhomogeneous assembly of contiguous distorted regions of roughly 4–6 nm extent (this roughly corresponds to the observed  $q$  width of the elastic satellites). Each region consists of alternating dark/light bands of  $\sim 1.2$  nm width parallel to either the  $(2\ 2\ 0)$  or  $(2\ \bar{2}\ 0)$  planes (viz., a quasiperiodicity of six  $\{220\}$  planes, where  $d_{220} \approx 0.2$  nm). This band width is the inverse of the satellite spacings found in reciprocal space. Below  $T_1$ , neutron scattering found that the satellite at  $\zeta_0$  become Bragg-like: its intensity increases dramatically, and the peak itself develops a structure, which corresponds to the mosaic spread of the crystal [Fig. 3(b)]. This structural development below room temperature has not been examined by TEM as yet.

The effects described above are in many ways similar to those observed in Ni-Al alloys,<sup>3</sup> though the phonon softening is even more pronounced in  $\text{Ni}_2\text{MnGa}$ . The  $\zeta = 0.325$   $[\zeta\zeta 0]$  TA<sub>2</sub> phonon energy squared versus temperature plot is shown on Fig. 5. In accordance with the original soft mode theory proposed by Cochran and Anderson,<sup>18</sup>  $(\hbar\omega)^2$  decreases linearly with temperature down to 260 K, but below this temperature it bends upwards again. The absence of complete phonon softening is phenomenologically accounted for by Landau-type theories developed by Krumhansl and Gooding<sup>19,20</sup> which include a homogeneous strain as an order parameter in addition to the periodic lattice distortion with the

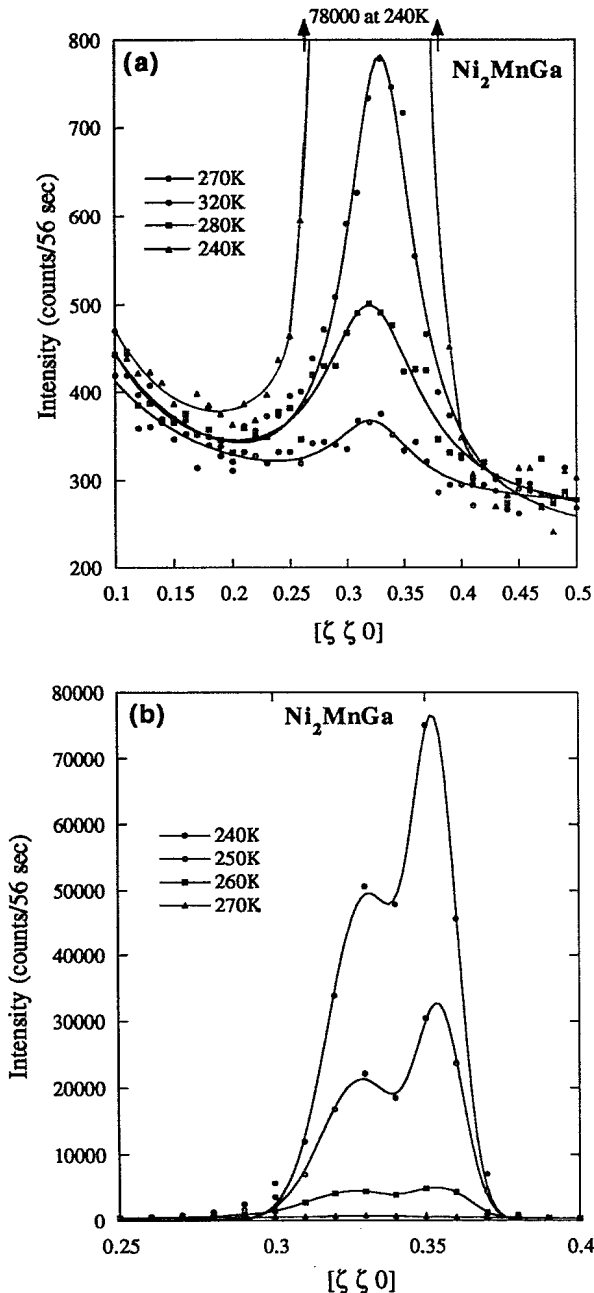


FIG. 3. Temperature dependence of the elastic scattering along  $[\zeta\zeta 0]$  (transverse) direction.

wave vector  $\zeta_0$ . Anharmonic coupling of these quantities may lead to a *thermodynamical* lattice instability and a first-order phase transition before the phonon driving the

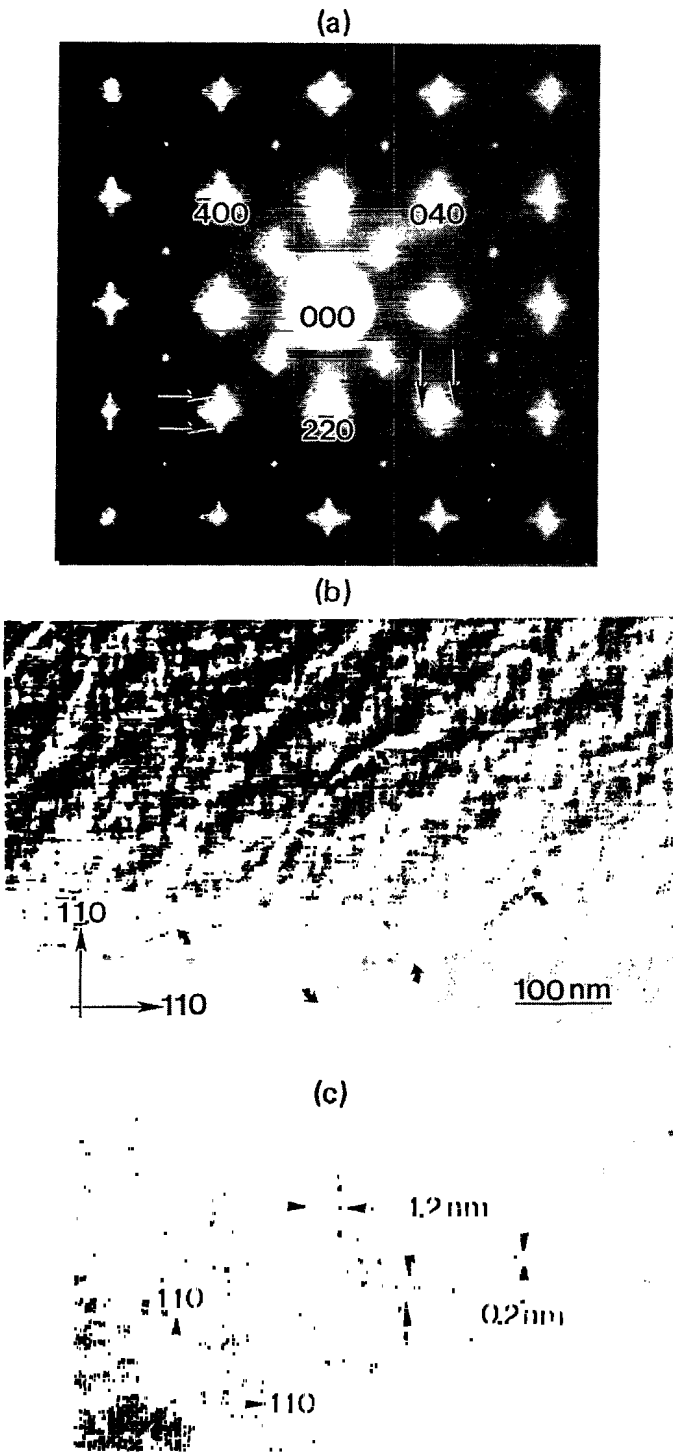


FIG. 4. (a) A symmetric (0 0 1) zone-axis electron diffraction pattern of the high-temperature parent L<sub>21</sub> structure obtained at 293 K; arrows indicate positions of satellites superimposed on the  $\langle \zeta \zeta 0 \rangle$  HDS streaks. (b) The CTEM microstructural image produced under two-beam bright-field condition; (001) orientation showing twinned strain contrast; arrows indicate antiphase boundaries in the ordered structure. (c) The HRTEM microstructural image showing local atomic displacements and micromodulated domain structure.

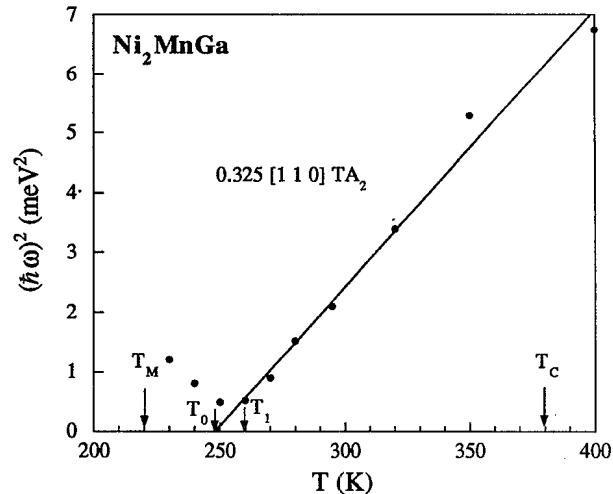


FIG. 5.  $(\hbar\omega)^2$  vs  $T$  for the  $[\zeta\zeta 0]$  TA<sub>2</sub> mode at  $\zeta = 0.325$ .

transition softens completely (i.e., before the lattice becomes *dynamically* unstable).

The micromodulated domains observed above  $T_1$  are direct evidence of the coupling of lattice defect strain fields with the softening of the elastic constant  $c'$  (homogeneous strain) and the phonon dip at  $\zeta_0$  (modulated strain) to produce shear-plus-shuffle strain fields that fall off with distance from the originating defects.<sup>3,17,19</sup> These “inhomogeneously strained domains” are effectively strain embryos generated by the weakest of lattice defects (e.g., vacancies, interstitials, misplaced solutes, etc.) and only become product phase nuclei if they are sufficiently potent (i.e., if the associated strain energy is sufficiently high) in relation to the height of the activation barrier.<sup>21</sup> Most martensitic alloy systems (e.g., Ni-Al, Ni-Ti, and most definitely steels) require stronger defects (dislocations, grain boundaries, the surface, etc.) to act as effective nucleation centers. The theory of heterogeneous nucleation as a function of defect potency coupled with lattice softening as  $T \rightarrow T_M$  has been treated recently by several investigators.<sup>22,23</sup>

The previous work on Ni<sub>2</sub>MnGa (Refs. 8 and 9) and some of our own observations seemed to indicate that the thermal transformation to the five-layer martensite from the premartensitic L<sub>21</sub> structure would be comparable to what was observed in Ni-Al alloys.<sup>3</sup> However, in Ni<sub>2</sub>MnGa the  $T$  intercept of a linear fit to the  $(\hbar\omega)^2$  vs  $T$  dependence is  $T_0 \approx 250$  K, which is *higher* than  $T_M$ . Therefore, an additional phase transition may be expected. Indeed, in the temperature range  $T_0 > T > T_M$  the L<sub>21</sub> structure should be dynamically unstable. As mentioned above, due to anharmonic effects a premartensitic phase may appear at temperatures higher than  $T_0$ . The dramatic increase in the intensity of the central peak, its shape in  $q$  space, and the increase of the soft mode frequency below  $T_1 \approx 260$  K confirm these speculations. Below  $T_1$  the elastic peaks at  $\zeta \approx 0.33$  correspond to Bragg scattering in the new phase. Though a more detailed investigation is required, one can say that the intermediate phase is approximately fcc (the principal L<sub>21</sub> Bragg peaks are practically unchanged, though their intensity decreases somewhat below  $T_1$ ), but a new mod-

ulation in the  $\{220\}$  system appears. This modulation corresponds to wave vector  $\zeta_0 = 0.33$  of the soft phonon and is completely different from the five-layer modulation in the close-packed martensitic phase ( $\zeta_M = 0.4$ ).

#### IV. CONCLUSION

Another system undergoing a martensitic phase transformation was studied by inelastic neutron scattering. Strong, nearly complete, phonon softening in the parent phase was shown to result in an additional phase transition to a transversely modulated structure with a periodicity corresponding to the soft mode wave vector. The phonon anomaly is not related to the magnetic ordering, and is probably due to electron-phonon interactions.

It would be interesting to see if first-principle calculations similar to those described in Refs. 4 and 5 could predict the observed phenomena. Further neutron scattering and electron microscopy experiments could clarify the structure of the intermediate phase and the effect of mechanical stress on the phase transformations.

#### ACKNOWLEDGMENTS

Work at Brookhaven National Laboratory was supported by the Division of Material Sciences, U.S. Department of Energy, under Contract No. DE-AC02-76CH00016. The work at Lawrence Livermore National Laboratory was performed under U.S. Department of Energy Contract No. W-7405-ENG-48.

- 
- <sup>1</sup> Z. Nishiyama, *Martensitic Transformations* (Academic, New York, 1978).
- <sup>2</sup> S. M. Shapiro, Y. Noda, Y. Fujii, and Y. Yamada, *Phys. Rev. B* **30**, 4314 (1984).
- <sup>3</sup> S. M. Shapiro *et al.*, *Phys. Rev. B* **44**, 9301 (1991).
- <sup>4</sup> G. L. Zhao *et al.*, *Phys. Rev. B* **45**, 7999 (1989).
- <sup>5</sup> G. L. Zhao and B. N. Harmon, *Phys. Rev. B* **45**, 2818 (1992).
- <sup>6</sup> P. J. Webster, K. R. A. Ziebeck, S. L. Town, and M. S. Peak, *Philos. Mag.* **49**, 295 (1984).
- <sup>7</sup> A. N. Vasil'ev, V. V. Kokorin, Y. I. Savchenko, and V. A. Chernenko, *Sov. Phys. JETP* **71**, 803 (1990).
- <sup>8</sup> V. V. Martynov and V. V. Kokorin, *J. Phys. (France) III* **2**, 739 (1992).
- <sup>9</sup> G. Fritsch, V. V. Kokorin, and A. Kempf, *J. Phys. Condens. Matter* **6**, L107 (1994).
- <sup>10</sup> R. D. Lowde *et al.*, *Proc. R. Soc. London A* **374**, 87 (1981).
- <sup>11</sup> M. Sato, B. H. Grier, S. M. Shapiro, and H. Miyajima, *J. Phys. F* **12**, 2117 (1982).
- <sup>12</sup> C. Zener, *Phys. Rev.* **71**, 846 (1947).
- <sup>13</sup> L. E. Tanner, *Philos. Mag.* **14**, 111 (1966).
- <sup>14</sup> L. E. Tanner, A. R. Pelton, and R. Gronsky, *J. Phys. (Paris) Colloq.* **43**, C4-169 (1982).
- <sup>15</sup> J. D. Axe, S. M. S. G. Shirane, and T. Riste, in *Anharmonic Lattice, Structural Transitions and Melting*, edited by T. Riste (Nordhoff, Leiden, 1974).
- <sup>16</sup> B. I. Halperin and C. M. Varma, *Phys. Rev. B* **14**, 4030 (1976).
- <sup>17</sup> D. Schryvers and L. E. Tanner, *Ultramicroscopy* **37**, 241 (1990).
- <sup>18</sup> *Structural Phase Transitions*, edited by A. D. Bruce and R. A. Cowley (Taylor and Francis, London, 1981).
- <sup>19</sup> J. A. Krumhansl and R. J. Gooding, *Phys. Rev. B* **39**, 3047 (1989).
- <sup>20</sup> J. A. Krumhansl, *Solid State Commun.* **84**, 251 (1992).
- <sup>21</sup> L. E. Tanner and M. Wuttig, *Mater. Sci. Eng. A* **127**, 137 (1990).
- <sup>22</sup> W. Cao, J. A. Krumhansl, and R. J. Gooding, *Phys. Rev. B* **14**, 11 319 (1990).
- <sup>23</sup> P. C. Clapp, *Physica D* **66**, 26 (1993).